EURO:TUN 2017, Innsbruck University, Austria

Influence of building geometry on bending and shear deformations of buildings subject to tunnelling subsidence: experimental testing

Stefan Ritter[1], Giorgia Giardina[2], Matthew J. DeJong[1] and Robert J. Mair[1]

[1]*Department of Engineering, University of Cambridge, United Kingdom*
[2]*Department of Architecture and Civil Engineering, University of Bath, United Kingdom*

Abstract: Tunnelling-induced settlement damage to pre-existing buildings is a result of bending and shear deformations, which typically occur simultaneously. However, widely accepted methods to assess building damage caused by tunnelling subsidence focus only on the mode of deformation (i.e. shear or bending) that is assumed to govern the onset of building damage. Furthermore, building damage assessment methods typically relate the dominant mode of deformation to the length to height ratio, L/H, of the structure, while more recent research reported that facade openings significantly affect the dominant deformation mode. This paper presents a series of centrifuge tests that explore bending and shear effects on surface structures that are affected by a shallow tunnel excavation in sand. The tests were performed on 3D printed building models with varying L/H ratio and facade openings. The response of these building models to the ground movements caused by the tunnelling operation is monitored using digital image correlation (DIC). Results show that bending deformations increase with the L/H ratio while shearing becomes dominant as the amount of facade openings increases. It is also shown that shearing and bending occur simultaneously and therefore should be combined in future damage assessment methods. The obtained experimental results provide essential benchmark data for computational modelling of tunnelling-induced settlement damage on surface structures, as presented in the companion paper.

1 INTRODUCTION

As the world continues to urbanise, there is an increasing demand for subsurface infrastructure solutions. The process of creating urban underground space, however, results in an interaction with the built environment, including the risk of tunnelling-induced building damage. It is therefore of utmost importance to understand how structures are responding to soil displacements caused by tunnelling or deep excavations.

Existing methods of assessing potential building damage due to tunnelling operation [1, 2, 3, 4] focus on the critical mode of deformation (i.e. bending or shear), which depends on the building geometry, i.e length to height ratio L/H [1, 5], and the presence of facade openings [5, 6]. These methods generally adopt deep beam theory and use the deflection ratio, Δ/L,

which is defined as the ratio between the relative vertical displacement to the length of the deflected part of the building, to account for building distortions. For masonry structures, with a frequently used Young's modulus to shear modulus ratio, E/G, of 2.6 [7], structures exceeding an L/H ratio of unity are reported to be more vulnerable to bending than to shear deformations [1]. By contrast, Boscardin & Cording [8] related the angular distortion, which is a measure of shear deformations, in combination with the horizontal strain to building damage. This approach was followed by Son and Cording [9], who showed that shear distortions control building damage of structures with a L/H ratio of 3-10. Additionally, these authors reported E/G values between 12 to 23 for masonry walls, which is in fair agreement with field observations reported by Cook [10]. This controversy about the critical mode of distortion (i.e. shear or bending) leads to significant amount of uncertainty when assessing building response to tunnelling-induced settlements.

This work sheds new light on the importance of taking shear and bending distortions into account when evaluating building response to tunnelling. Experimental results of a centrifuge modelling study, replicating soil-structure interaction during tunnel excavation, are presented. The section that follows briefly introduces the methodology, after which effects of changing L/H and facade openings on the shear and bending response of structures to tunnelling subsidence are highlighted.

2 METHODOLOGY

Geotechnical engineering experiments provide essential data to validate computational models. However, the soil behaviour is a function of the current stress state, and small-scale models tested at 1g cannot reproduce the conditions experienced in the field. Centrifuge modelling overcomes this problem by replicating the self-weight soil stresses of a prototype by increasing the gravitational field acting on a reduced scale model and has been used to explore tunnelling effects on the built environment [11].

In this study centrifuge modelling was used to simulate a shallow tunnelling project in dense sand (Fig. 1). In comparison to previous work, building models were 3D printed to reproduce important building characteristics at a scale of 1:75. To replicate the prototype self-weight stresses of the building and the ground, the centrifuge model was accelerated to 75 g. Building and ground displacements were monitored by an image based deformation measurement technique [13]. The main components of the experimental model are detailed below, after which the different urban tunnelling scenarios modelled are presented.

2.1 Modelling the tunnel excavation

A schematic plane strain tunnel excavation was simulated by reducing the tunnel diameter in a controlled manner. With respect to a real tunnelling operation, this modelling technique replicates ground movements caused by shield loss, tail void loss and lining deflection loss. Ground movements caused by face loss are neglected; consequently, this technique is more feasible to simulate closed face tunnelling. The main components of the model tunnel are a

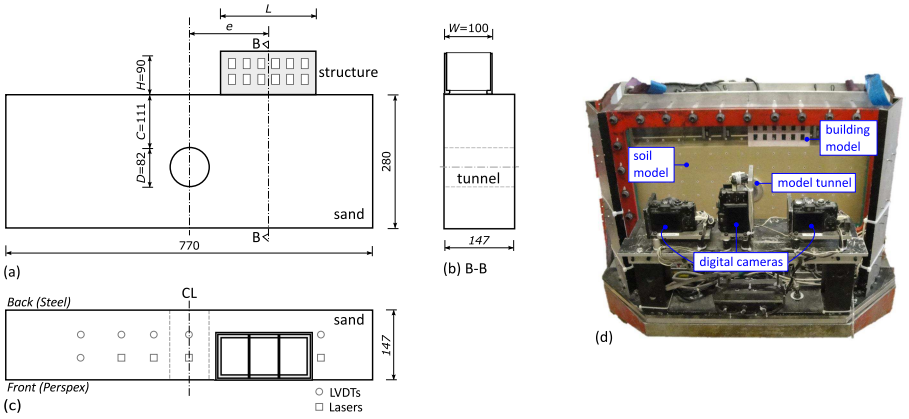

Figure 1: Small-scale centrifuge model (dimensions in mm).

brass cylinder and a latex membrane. The cavity between the latex membrane and the brass cylinder is filled with water, which is incrementally drained to achieve tunnel volume loss, $V_{l,t}$. This technique allows various tunnel volume loss increments to be studied within a single centrifuge test.

2.2 Soil conditions

Soft ground tunnelling conditions were modelled by air pluviation of Leighton Buzzard Fraction E silica sand to a relative density, I_R, of 90% ($\pm$3%). The main characteristics of this sand type are an average grain size, D_{50}, of 0.15 mm, an uniformity coefficient, U_c, of 1.58, a specific gravity, G_s, of 2.67, a minimum, e_{min}, and maxim void ratio, e_{max}, of 0.613 and 1.014 and a critical state friction angle, ϕ_{crit}, of 32° [14].

2.3 Modelling the surface structures

The building models were 3D printed to create structural models with representative building layout and characteristics, as shown in Figure 2. A Zprinter 350 with Visijet PXLCore powder and Visijet PXLClear binder was used. An additional surcharge in form of dead load bars (Fig. 2a) was placed on top of the structural model to obtain a soil-structure stress of 100 kPa beneath the footings perpendicular to the tunnel. The main advantage of employing 3D printing was that building features such as partitioning walls, strip footings and window openings could be replicated at a scale of 1:75.

Rectangular specimens were printed in every print job and tested in 4-point bending to determine the material properties of the 3D printed material. The obtained Young's modulus, E, was in the range of masonry while the 3D printed material had a lower density, ρ, and higher flexural strength, f_t, and ultimate strain to failure, ϵ_{ult}. The dimensions of the various buildings tested were selected to obtain a realistic range of building bending stiffness values for real case study buildings. Further details of the experimental setup are given in [15].

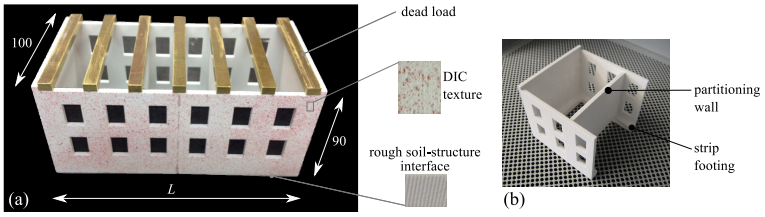

Figure 2: Building model (dimensions in mm).

2.4 Urban tunnelling scenarios

Figure 3 presents the modelled urban tunnelling scenarios. While the ground and tunnelling configurations were kept constant throughout this test series, building characteristics, including the building position relative to the tunnel, e, the building length, L, and the amount of window openings, O, varied.

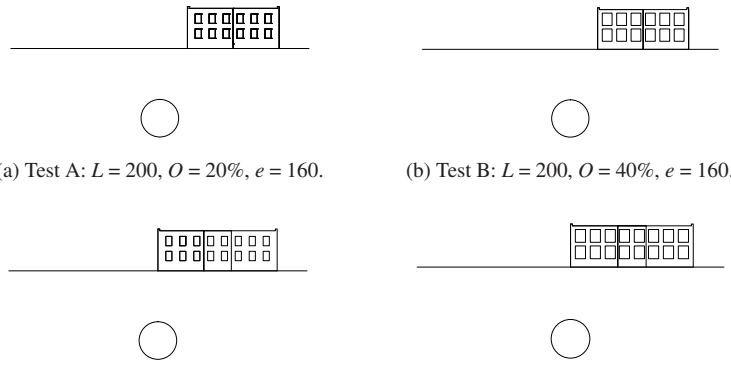

(a) Test A: L = 200, O = 20%, e = 160.

(b) Test B: L = 200, O = 40%, e = 160.

(c) Test C: L = 260, O = 20%, e = 130.

(d) Test D: L = 260, O = 40%, e = 130.

Figure 3: Urban tunnelling scenarios (L and e in mm).

3 RESULTS

To distinguish between the bending and shear deflections caused by tunnelling subsidence, the framework outlined by Cook [10] was adopted. Figure 4 defines the sign convention, the definition of the bending and tilt deflections and the subdivision of buildings at the position of their transverse walls. For each bay the following steps were carried out.

Firstly, the displacement due to tilt was defined as

$$\Delta y_{tilt} = sin(\omega_2) \cdot L \ . \tag{1}$$

Secondly, the bending deflection was derived as

$$\Delta y_{bend} = tan(\omega) \cdot L \tag{2}$$

where positive values of Δy_{bend} indicate a hogging (i.e. convex) mode of deflection. Thirdly, the total vertical displacement was computed as

$$\Delta y_{tot} = \Delta y_A - \Delta y_B \ . \tag{3}$$

Finally, the shear deflection was defined as

$$\Delta y_{shear} = \Delta y_{tot} - \Delta y_{tilt} - \Delta y_{bend} \ . \tag{4}$$

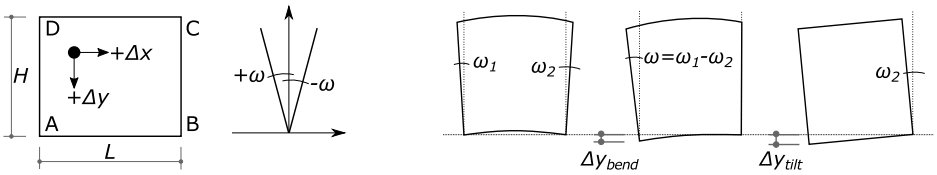

(a) Reference condition for a single building bay and sign convention.

(b) Bending and tilt deflection.

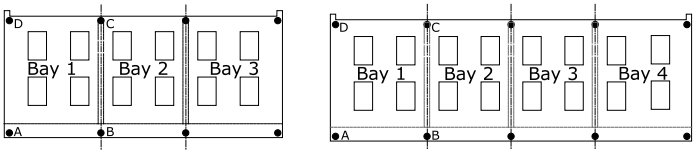

(c) Separation of buildings into bays.

Figure 4: Framework to investigate building response.

Figure 5 compares the different displacement and deflection components (see above) along $V_{l,t}$ for test A (Fig. 3). In addition to the acquired data, the solid lines represent 2^{nd} order polynomials fitted to the data. For all tests, the displacements became larger as $V_{l,t}$ increased. The largest total displacements were monitored in Bay 1 and reduced with distance from the tunnel (i.e. Bay 2 and 3). Rigid body rotation, measured as tilt, stayed rather equal for the different building bays, indicating a substantial rotation of the entire structure towards the tunnel. Interestingly, the deflection due to tilt exceeded the total displacement obtained in Bay 3 (Fig. 5c). This observation might be explained by reduced vertical displacements in Bay 3 due to a narrower tunnelling-induced settlement trough as $V_{l,t}$ increased.

While the total displacements and the the tilt might cause serviceability concerns, the deflection due to bending and shear can be related to tensile strains, and thus are of main importance when assessing potential building damage. For the bays of test A, a small bending contribution was measured whereas notable shear deflections were obtained for Bay 1 and 3. These results reveal the important contribution of the shearing component. Although the entire extent of the building model of test A was placed in the hogging zone of the corresponding greenfield settlement profile, only in Bay 1 a hogging deformation (i.e. positive Δy_{bend}) was observed. At lower $V_{l,t}$, Bay 2 and 3 responded in sagging while a hogging mode of deformation became evident with increasing $V_{l,t}$. Very similar trends were observed for the tests B, C and D. However, due to space limitations these results are not explicitly presented herein,

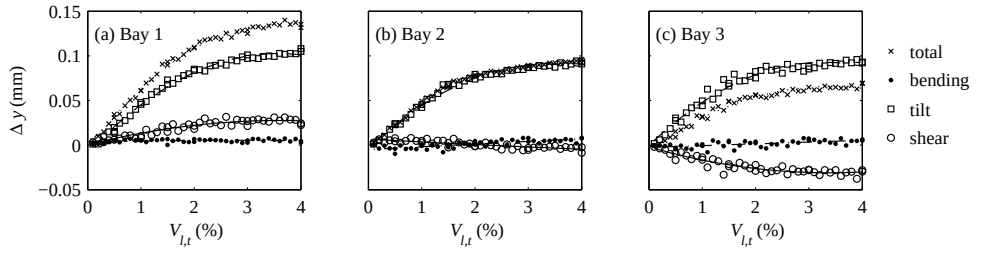

Figure 5: Total displacements and tilt, bending and shear components versus tunnel volume loss for test A.

but are used below to quantify effects of building dimensions and facade openings on shear and bending deformations.

Figure 6 presents the impact of the building dimensions on the bending and shear deflections. The analysed bays (i.e. Bay 1 for buildings with L = 200 mm and Bay 2 for building with L = 260 mm) have an equal location relative to the tunnel. For different amount of window openings (i.e. 20% and 40%) an increase of the building length from 200 mm to 260 mm caused greater bending deflections while shear deflections kept rather equal. This is particularly true as $V_{l,t}$ increases, and the substantial change of bending and shear deflection in test D indicates cracking initiation at a $V_{l,t}$ of about 2.5% (Fig. 6b and 6d). Although L/H increased only from 2.2 to 2.9, an increase of the building length combined with the position of the building in hogging and sagging lead to a substantially higher risk of building damage.

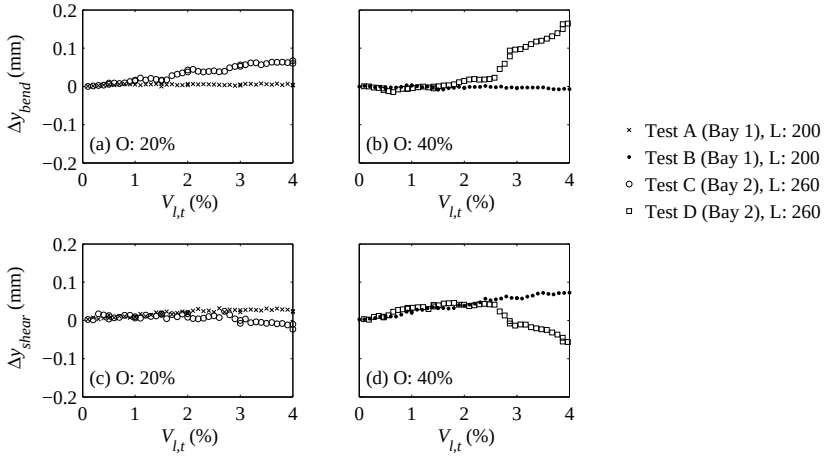

Figure 6: Influence of increasing *L/H* on bending and shear deflections.

Figure 7 shows the shear and bending deflection along tunnel volume loss for different amount of window openings while the building length was kept constant. As indicated in Figure 7b, data from equal building bays are compared within a subplot. For buildings with

different length and thus different position relative to the tunnelling-induced settlement profile, an increase of window openings from 20% to 40% caused greater shear deflections while the bending components generally remained close to zero. Only in Bay 2 of the structures with L = 260 mm a considerable bending contribution was measured.

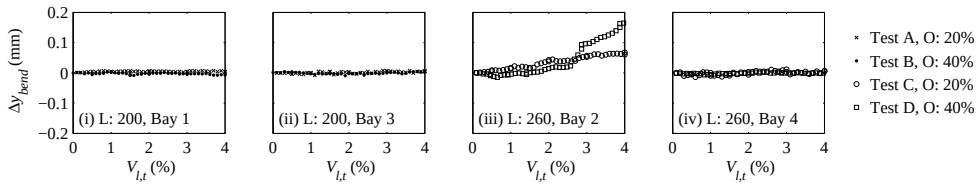

(a) Bending deflections.

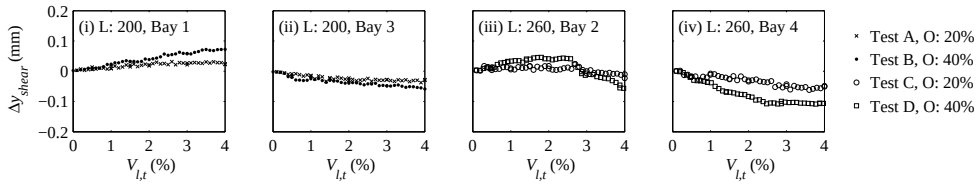

(b) Shear deflections.

Figure 7: Influence of increasing the opening percentage on bending and shear deflections.

4 CONCLUSIONS

The main goal of this study was to experimentally determine the bending and shear deformation components of buildings subject to tunnel excavation. The results have shown how shear and bending deformations vary throughout the length of the buildings.

The experimental data was used to evaluate the effect of changing building dimensions and facade opening percentage on the bending and shear deformations. An increase of the building length lead to an increase of bending deflections while shear deflections remained rather equal. By contrast, a larger amount of window openings caused a considerable increase of the shear component but had little affect on bending deformations. These findings indicate the importance of considering both shear and bending deformations when assessing tunnelling-induced settlement damage on structures.

Acknowledgments

The authors are grateful to EPSRC grant EP/KP018221/1 and Crossrail for providing financial support. The related research data is available at https://doi.org/10.17863/CAM.6475.

References

[1] J. B. Burland, and C. Wroth, *Settlement of buildings and associated damage*, Proceedings of Conference on Settlement of Structures, Cambridge, United Kingdom, (Pentech Press, 1974).

[2] D. M. Potts, and T. I. Addenbrooke, *A structure's influence on tunnelling-induced ground movements*, Proc. Instn. Civ. Engrs. Geotech. Engng. **125** (1997) 109-125.

[3] J. N. Franzius, D. M. Potts, and J. B. Burland, *The response of surface structures to tunnel construction*, Proc. Instn. Civ. Engrs. Geotech. Engng. **159** (2006) 3-17.

[4] K. H. Goh, and R. J. Mair, *The response of buildings to movements induced by deep excavations*, Geot. Eng. Journ. of the SEAGS and AGSSEA. **42(3)** (2011).

[5] J. A. Pickhaver, J. H. Burd and G. T. Houlsby, *An equivalent beam method to model masonry buildings in 3D finite element analysis*, Computers & Structures **88** (2006) 1049-1063.

[6] M. Melis, and J. Rodriguez Ortiz, *Consideration of the stiffness of buildings in the estimation of subsidence damage by EPB tunnelling in the Madrid subway*, In Resp. Build. to Exc. Ind. Gr. Mov. Conf., London, United Kingdom (2001).

[7] R. J. Mair, R. N. Taylor and J. B. Burland, *Prediction of ground movements and assessment of risk of building damage due to bored tunnelling*, Proc. Geot. Asp. of Und. Const. in Soft Ground, Balkema, Rotterdam (1996) 713-718.

[8] N. D. Boscardin, and E. J. Cording, *Building Response to Excavation-Induced Settlement*, ASCE J. of Geot. Eng. **115(1)** (1989) 1-21.

[9] M. Son, and E. J. Cording, *Evaluation of building stiffness for building response analysis to excavation-induced ground movements*, ASCE J. of Geot. Eng. **133(8)** (2007) 995-1002.

[10] D. Cook, *Studies of settlements and crack damage in old and new facades*, Proceedings 3rd Int. Masonry Conference, London. United Kingdom, Vol. 6. (1974)).

[11] R. P. Farrell, and R. J. Mair, *Centrifuge modelling of the response of buildings to tunnelling*, Proc. Geot. Asp. of Und. Const. in Soft Ground, Rome, Italy, (CRC Press, 2011).

[12] G. Giardina, M. J. DeJong, and R. J. Mair, *Interaction between surface structures and tunnelling in sand: Centrifuge and computation modelling*, TUST **50** (2015) 465-478.

[13] D. J. White, A. W. Take and M. D. Bolton, *Soil deformation measurement using particle image velocimetry (PIV) and photogrammetry*, Geotechnique **53(7)** (2003) 619-632.

[14] S. K. Haigh, and G. S. P. Madabhushi, *Dynamic centrifuge modelling of the destruction of Sodom and Gomorrah*, Proc. Int. Conf. Phys. Mod. in Geot., St John's Newfoundland, Canada, (2002).

[15] S. Ritter, G. Giardina, M. J. DeJong, and R. J. Mair, *Centrifuge modelling of building response to tunnel excavation*, Int. J. Ph. Mod. in Geot. - Manuscript submitted for review (2017) .